

1 **Enhancement of Photoelectrochemical Activity of SnS Photoelectrodes using TiO<sub>2</sub>,**  
2 **Nb<sub>2</sub>O<sub>5</sub>, and Ta<sub>2</sub>O<sub>5</sub> Metal Oxide Layers**

3

4 Junie Jhon M. Vequizo<sup>1</sup>, Masanori Yokoyama<sup>1</sup>, Masaya Ichimura<sup>2</sup>, and Akira Yamakata<sup>1,3\*</sup>

5 <sup>1</sup>Quantum Interface Laboratory, Graduate School of Engineering, Toyota Technological Institute, 2-12-1 Hisakata,  
6 Tempaku, Nagoya 468-8511, Japan

7 <sup>2</sup>Department of Engineering Physics, Electronics, and Mechanics, Nagoya Institute of Technology, Gokiso, Showa, Nagoya  
8 466-8555, Japan

9 <sup>3</sup>Precursory Research for Embryonic Science and Technology (PRESTO), Japan Science and Technology Agency (JST), 4-  
10 1-8 Honcho Kawaguchi, Saitama 332-0012, Japan

11

12 **Abstract**

13 SnS fine photoelectrode fabricated by 3-step pulsed electrodeposition was active for H<sub>2</sub> evolution.  
14 The incident-photon-conversion-efficiency (IPCE) increases from 900 nm and is in good fit with the  
15 absorption spectrum. The activity was enhanced 3.4, 3.0, and 1.8 times higher than bare SnS by loading  
16 Nb<sub>2</sub>O<sub>5</sub>, TiO<sub>2</sub>, and Ta<sub>2</sub>O<sub>5</sub>, respectively. Nb<sub>2</sub>O<sub>5</sub> was most efficient because its conduction band is low  
17 enough for the effective electron transfer from SnS, but also has enough high-potential for H<sub>2</sub> evolution.  
18 The overall activity is determined by the competitive interfacial electron transfer between SnS/metal-  
19 oxide and metal-oxide/water. Therefore, construction of appropriate heterojunction is necessary for the  
20 further improvement of photoelectrochemical systems.

21

22 \*Corresponding Author: yamakata@toyota-ti.ac.jp

23

1 Water splitting reaction has gained great attention due to its clean and environmentally friendly  
2 approach to generate hydrogen gas by utilizing solar energy. Photoelectrochemical (PEC) system  
3 involving semiconductor electrodes is one of the feasible methods to produce hydrogen gas. For the  
4 development of PEC system, a suitable choice of semiconducting electrodes is necessary. The  
5 conduction band and valence band of the semiconductor should be located at more negative and  
6 positive than the reduction potential of H<sub>2</sub>O (0 V vs SHE) and oxidation potential of H<sub>2</sub>O (1.23 V vs  
7 SHE), respectively.<sup>1</sup>

8 Metal sulfides with p-type conductivity such as copper indium gallium sulfide (CIGS), copper indium  
9 sulfide (CIS), and tin sulfide (SnS) are expected to be promising candidates for H<sub>2</sub> gas generation.  
10 These sulfides are studied for solar cells and photoelectrochemical cells. Among these sulfides, SnS is  
11 relatively easy to fabricate. Moreover, it has high absorption coefficient,  $\alpha > 10^4 \text{ cm}^{-1}$ ,<sup>2</sup> and strongly  
12 absorbs visible and near IR light up to 900 nm. Furthermore, the conduction band of SnS is located at -  
13 1.22 V vs SHE at pH = 0, which is more negative than the potential of water reduction.<sup>3</sup> SnS has been  
14 utilized as an absorber layer in solar cells, but its application in photoelectrochemistry has not been  
15 reported to the best of our knowledge.

16 Loading of metal oxide is often used to protect the photoelectrodes from photocorrosion.  
17 Especially, photoanodes made of metal sulfides and nitrides are readily oxidized in anodic conditions.  
18 The metal oxides are stable and they can therefore protect the electrodes from photocorrosion.  
19 Furthermore, for photoelectrodes fabricated from the powder particles by thermal sintering, metal  
20 oxides provide effective contacts between particles, hence promoting inter-particle charge transfer by  
21 the so called “necking effects”. Therefore, metal oxides such as TiO<sub>2</sub>, Ta<sub>2</sub>O<sub>5</sub>, ZnO, and Al<sub>2</sub>O<sub>3</sub> are used  
22 to cover the n-type semiconductors such as ZnO<sup>4</sup>, GaAs<sup>5</sup>, LaTiO<sub>2</sub>N<sup>6</sup>, TaON, and Ta<sub>3</sub>N<sub>5</sub>.<sup>7,8</sup> Metal  
23 oxides are also useful to protect photocathodes, although the photocathodes are relatively stable in the  
24 cathodic condition. TiO<sub>2</sub> has been used as protective layers of photocathodes such as p-Si, p-GaAs<sup>9</sup>, p-  
25 Cu<sub>2</sub>O<sup>10,11</sup>, p-InP<sup>12</sup>, and p-Cu<sub>2</sub>ZnSnS<sub>4</sub>,<sup>13</sup> and several authors proposed that TiO<sub>2</sub> would enhance the  
26 charge separation at the electrode/TiO<sub>2</sub> interface. As the position of the CB of the loaded metal oxides  
27 becomes lower, the electron transfer from electrode to the metal oxides is enhanced. However, the  
28 reactivity of electrons in the metal oxides becomes lower. In the case of TiO<sub>2</sub>, the height of the CB is  
29 not sufficiently high compared to the potential for water reduction; therefore TiO<sub>2</sub> would not be always  
30 the best material for the effective H<sub>2</sub> evolution reaction. We therefore expect that a more suitable  
31 material other than TiO<sub>2</sub> should be highly considered to enhance the H<sub>2</sub> evolution; however the

1 application of other metal oxides such as Nb<sub>2</sub>O<sub>5</sub> and Ta<sub>2</sub>O<sub>5</sub> to p-type semiconductors has not been  
2 systematically studied as far as we know.

3 In this work, we fabricated p-type SnS thin film electrodes and examined the effects of metal-oxide  
4 loading on the photoelectrochemical activity. TiO<sub>2</sub>, Nb<sub>2</sub>O<sub>5</sub>, and Ta<sub>2</sub>O<sub>5</sub> were loaded on SnS, and we  
5 found that all of them enhanced the PEC activity of SnS photocathode for H<sub>2</sub> evolution. Among these  
6 metal oxides, Nb<sub>2</sub>O<sub>5</sub> was most effective to enhance the activity. The favorable position of the  
7 conduction band of the metal oxide with respect to SnS is responsible for the enhancement.

8 SnS thin film photoelectrodes were fabricated by electrodeposition technique onto the ITO-  
9 coated glass following the procedure developed by Prof. Ichimura and co-workers.<sup>14-16</sup>  
10 Electrodeposition method has been considered as one of the attractive methods to produce smooth, flat,  
11 and high quality oxides<sup>17-23</sup> and sulfides<sup>14,24,25</sup> thin films owing to its simplicity, feasibility at room  
12 temperature operation, and easy scalability. It has also been utilized for the fabrication of  
13 heterojunction structures for solar cells.<sup>26,27</sup> Especially, pulse electrodeposition method produces denser  
14 and smoother SnS compared to DC (one-step potential) electrodeposition.<sup>16</sup> As evidenced in the PEC  
15 experiment, the pulse electrodeposited SnS exhibited 3-fold increase of photocurrent compared to DC  
16 electrodeposited SnS (Figure S1). Therefore, a 3-step pulsed potential ( $V_1 = -1.0$ ,  $V_2 = -0.6$ , and  $V_3 = 0$   
17 V vs Ag/AgCl) was employed to deposit SnS thin films onto the ITO substrate (1 x 1 cm<sup>2</sup> area). The  
18 pulse duration for each potential was fixed at 10 s and the total deposition time was maintained at 10  
19 min. The mixture of SnSO<sub>4</sub> (30 mM) and Na<sub>2</sub>S<sub>2</sub>O<sub>3</sub> (100 mM) aqueous solution was used as precursor  
20 solution. The detailed reaction of these Sn and S precursors to produce SnS was reported elsewhere.<sup>14,15</sup>  
21 The chemical composition was characterized by Auger electron spectroscopy (JEOL JAMP-9500F)  
22 and X-ray photoelectron spectroscopy (XPS PHI-5000, ULVAC-PHI), and the optical absorption of the  
23 as-prepared SnS film were measured by UV-VIS absorption spectrometer (JASCO V-670),  
24 respectively.

25 For the SnS electrodes loaded with TiO<sub>2</sub>, Nb<sub>2</sub>O<sub>5</sub>, and Ta<sub>2</sub>O<sub>5</sub>: TiCl<sub>4</sub>, NbCl<sub>5</sub>, and TaCl<sub>5</sub> ethanol  
26 solution (10 mM) was dropped on the SnS film, respectively. The deposited metal ions react with water  
27 vapor in air to produce the metal oxide thin layer on SnS. For photoelectrochemical (PEC)  
28 measurement, the electrodes were irradiated from the substrate side by using 660 nm-LED lamp  
29 (Thorlabs, M660L3) with a power density of 200 mW cm<sup>-2</sup>. The resulting photocurrent response under  
30 intermittent irradiation was measured in 0.1 M NaSO<sub>4</sub> aqueous solution, which was deaerated with Ar  
31 gas bubbling prior to each measurement. The potential was linearly scanned from +0.2 to -1.0 V vs  
32 Ag/AgCl at a rate of 10 mV s<sup>-1</sup>.

1 The composition of the SnS photoelectrode deposited by 3-step pulsed electrodeposition was  
2 characterized by Auger electron spectroscopy. The Auger differential spectrum (Figure S2) clearly  
3 shows that the Sn and S peaks are nearly stoichiometric Sn/S ratio. The composition of the film was  
4 further analyzed by X-ray photoelectron spectroscopy (Figure S3). The binding energies of Sn 3d and S  
5 2p peaks indicate that the film is mainly SnS. The band gap was estimated to be 1.4 eV from the  
6 absorption edge at 880 nm (Figure S4). The SnS film consists of aggregated particles (Figure S5a), and  
7 the thickness was estimated to be around 2.2  $\mu\text{m}$  in our previous experiments.<sup>15</sup> The photocurrent  
8 response of bare SnS electrode was measured under 660 nm intermittent irradiation from +0.2 to -1.0 V  
9 (Figure 1a). The photocurrent of the SnS electrode was clearly observed upon irradiation, i.e. the  
10 cathodic current was observed below -0.2 V. At more negative potentials, the photocurrent was further  
11 increased. This cathodic current is ascribed to water reduction producing  $\text{H}_2$  gas. This result also  
12 confirms us that SnS has p-type conductivity.

13 Figure 1b shows the incident-photon-energy-conversion (IPCE) curve of SnS photoelectrode  
14 measured at an applied potential of -0.6 V. As seen in the figure, the IPCE gradually increases from  
15 900 nm towards shorter wavelength, and it is in good agreement with the absorption spectrum. The  
16 conversion efficiency at 400 nm is estimated to be 10.8 %. These results, therefore, indicate that the  
17 observed cathodic current is due to the band gap photoexcitation of SnS, i.e. SnS converts photons into  
18 current for  $\text{H}_2$  gas generation.

19 We then examined the effect of metal oxides ( $\text{TiO}_2$ ,  $\text{Nb}_2\text{O}_5$ , and  $\text{Ta}_2\text{O}_5$ ) loadings on the activity of  
20 SnS electrode. These metal oxides are chemically stable and optically transparent to visible and near-IR  
21 light. The morphologies of  $\text{TiO}_2$ ,  $\text{Nb}_2\text{O}_5$ , and  $\text{Ta}_2\text{O}_5$  loaded SnS look very similar to that of bare SnS  
22 (Figure S5). To confirm whether the loaded metal oxide covers the SnS surface, we further performed  
23 elemental mapping by EDX. For brevity, the elemental mapping of  $\text{Nb}_2\text{O}_5$  loaded SnS was only  
24 presented (Figure S6). As seen in the figure, it looks like the  $\text{Nb}_2\text{O}_5$  fully covered the SnS film, but we  
25 could not exclude the possibility that pinholes are formed in the SnS particles.

26 By  $\text{TiO}_2$  loading (Fig. 2b), the photocurrents increased by 3 times ( $547 \text{ mA}/\text{cm}^2$ ) compared to that  
27 obtained for bare SnS ( $183 \text{ mA}/\text{cm}^2$ ) at -0.76 V. In the case of  $\text{Nb}_2\text{O}_5$  loading (Fig. 2c), the cathodic  
28 current further increased by nearly 3.4 times ( $620 \text{ mA}/\text{cm}^2$ ) at the same applied potential. However, in  
29 the case of  $\text{Ta}_2\text{O}_5$  loading (Fig. 2c), the cathodic current only increases by 1.8 times ( $320 \text{ mA}/\text{cm}^2$ )  
30 compared to that of bare SnS at -0.76 V. The efficiency of charge separation and the reactivity of

1 electrons in the metal oxides are responsible for the difference in the degree of photocurrent  
2 enhancement as will be discussed later. Nevertheless, these results suggest that loading of metal oxides  
3 such as  $\text{TiO}_2$ ,  $\text{Nb}_2\text{O}_5$ , and  $\text{Ta}_2\text{O}_5$  improve the activity of SnS photocathodes, but the degree of  
4 enhancement depends on the metal oxides used for coatings. The dependence of the photocurrent  
5 enhancement on the thickness of metal oxide layer was also examined. The thickness of the metal  
6 oxides loaded on SnS was estimated and listed in Table S1 (Supporting Information). As shown in  
7 Figure S7, the increased of photocurrent is almost constant at  $\sim 50 \mu\text{L}$  loading, indicating that the  
8 enhancement is less sensitive to the amount of metal oxides loaded on SnS.

9 The properties of metal oxide layers fabricated by hydrolysis of metal chlorides are further  
10 examined by XRD. No characteristic peaks associated to crystalline  $\text{TiO}_2$ ,  $\text{Nb}_2\text{O}_5$ , and  $\text{Ta}_2\text{O}_5$  were  
11 observed in the XRD patterns for all the samples, suggesting that these oxide layers are in amorphous  
12 phase (Figure S8). However, their band gap energies are different. From the absorption edges of the  
13 UV-Vis absorption spectra in Fig. 3, the band gaps are estimated to be 3.2 (385 nm), 3.4 (360 nm), and  
14 4.1 eV (300 nm) for  $\text{TiO}_2$ ,  $\text{Nb}_2\text{O}_5$ , and  $\text{Ta}_2\text{O}_5$ , respectively. The positions of CB and VB of metal  
15 oxides are identified in referenced to the reported band structures of  $\text{TiO}_2$ ,  $\text{Nb}_2\text{O}_5$ , and  $\text{Ta}_2\text{O}_5$ .<sup>3,28-30</sup> In  
16 the case of  $\text{TiO}_2$ , the VBM and CBM are located at +3.0 and -0.2 eV from the hydrogen evolution  
17 potential. In the case of  $\text{Nb}_2\text{O}_5$ , the VBM is also located near to +3.0 eV. Since the band gap of  $\text{Nb}_2\text{O}_5$   
18 is higher than  $\text{TiO}_2$  by 0.2 eV, then the CBM is positioned at -0.4 eV above the hydrogen evolution  
19 potential. In the case of  $\text{Ta}_2\text{O}_5$ , the VBM is located at +3.0 - 3.5 eV in referenced to the hydrogen  
20 evolution potential. The slight difference depends on the method of measurement as reported in the  
21 literatures. Since the CB of these oxides are lower than that of SnS, the photoexcited electrons in SnS  
22 will migrate to these oxides layers, leaving the holes in SnS. This effective charge separation would be  
23 the primary reason why the activity is enhanced by metal-oxide loading on SnS. We found that  $\text{Nb}_2\text{O}_5$   
24 is most effective for  $\text{H}_2$  evolution. This mechanism can be explained as follows. The efficiency of the  
25 charge separation between SnS and oxides becomes higher as the CB of oxides becomes lower.  
26 Therefore, the efficiency of the charge separation becomes higher in the order of  $\text{TiO}_2$ ,  $\text{Nb}_2\text{O}_5$ , and  
27  $\text{Ta}_2\text{O}_5$ . However, this order is opposite for the reactivity of electrons in CB: it is higher in the order of  
28  $\text{Ta}_2\text{O}_5$ ,  $\text{Nb}_2\text{O}_5$ , and  $\text{TiO}_2$ . In the case of  $\text{TiO}_2$ , CB is lowest; therefore the efficiency of the charge  
29 separation is highest. However, the conduction band of  $\text{TiO}_2$  is almost comparable with that of redox  
30 potential for  $\text{H}_2$  evolution; hence the activity for the  $\text{H}_2$  evolution is lowest. In the case of  $\text{Nb}_2\text{O}_5$ , the  
31 height of the CB is adequate for the effective charge separation and the electrons have enough potential

1 for H<sub>2</sub> evolution. These are the reasons why Nb<sub>2</sub>O<sub>5</sub> shows higher activity for H<sub>2</sub> evolution than TiO<sub>2</sub>.  
2 On the contrary, in the case of Ta<sub>2</sub>O<sub>5</sub>, CB is highest therefore the reactivity of electrons is highest, but  
3 the efficiency of charge separation is lowest. These findings suggest that the overall activity is  
4 determined by the competition between the efficiency of charge separation and the reactivity of  
5 electrons.

6 In this work, we have fabricated fine SnS thin film electrodes by 3-step pulsed electrodeposition,  
7 and examined the photoelectrochemical activity. It is found that SnS is active for H<sub>2</sub> evolution under  
8 illumination of visible and NIR light shorter than 900 nm. The photoelectrochemical activity of SnS  
9 was much improved by loading metal oxides such as TiO<sub>2</sub>, Nb<sub>2</sub>O<sub>5</sub>, and Ta<sub>2</sub>O<sub>5</sub>. TiO<sub>2</sub> has been often  
10 used as protective layers to suppress photocorrosion of unstable electrodes,<sup>31-33</sup> and several authors  
11 proposed that TiO<sub>2</sub> also enhances the charge separation at the heterojunction. In the present case, the  
12 enhancement of the charge separation would be also responsible for the improved activity. However,  
13 we found that Nb<sub>2</sub>O<sub>5</sub> exhibited the highest activity among the metal oxides examined here. This  
14 activity enhancement depends on the height of the CB of metal oxides, which determines the efficiency  
15 of charge separation at the SnS/metal-oxide heterojunction as well as the reactivity of electrons for H<sub>2</sub>  
16 evolution on the metal oxides. The overall activity is determined by the competitive interfacial electron  
17 transfer between SnS/metal-oxide and metal-oxide/water. These findings suggest that the construction  
18 of appropriate band structures between SnS and metal oxide layers can further improve the activity for  
19 H<sub>2</sub> evolution reaction.

20 This work was supported by the PRESTO/JST program, the Grant-in-Aid for Specially Promoted  
21 Research (No. 23000009) and Basic Research (B) (No. 23360360), and the Strategic Research  
22 Infrastructure Project of MEXT. The authors would like to thank Mr. Yukihiisa Moriguchi of Nagoya  
23 Institute of Technology for his technical assistance in XPS measurement and Dr. Sampath Ranasinghe  
24 of Toyota Technological Institute for his assistance in EDX measurement.

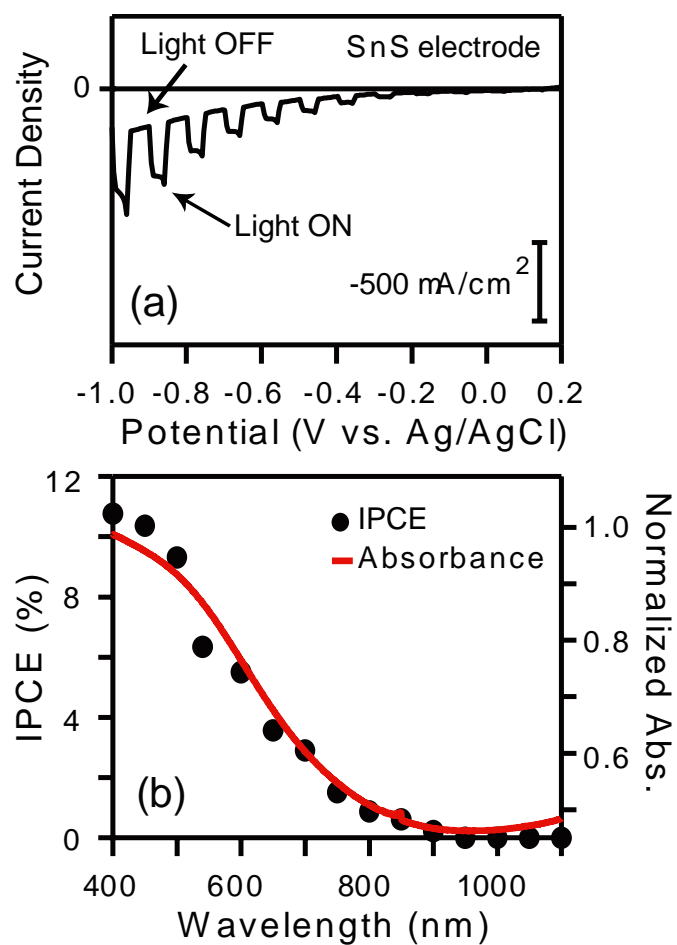
25

- 1 1 M. G. Walter, E. L. Warren, J. R. McKone, S. W. Boettcher, Q. Mi, E. A. Santori, and N. S. Lewis, *Chem. Rev.* 110, 6446 (2010).
- 2 2 N. K. Reddy and K. T. R. Reddy, *Physica B Condens. Matter* 368, 25 (2005).
- 3 3 C. Y. Yang, W. D. Wang, Z. C. Shan, and F. Q. Huang, *J. Solid State Chem.* 182, 807 (2009).
- 4 4 C. Li, T. Wang, Z. Luo, D. Zhang, and J. Gong, *Chem. Commun.* 51, 7290 (2015).
- 5 5 M. Tomkiewicz and J. M. Woodall, *J. Electrochem. Soc.* 124, 1436 (1977).
- 6 6 N. Nishimura, B. Raphael, K. Maeda, L. Le Gendre, R. Abe, J. Kubota, and K. Domen, *Thin Solid Films* 518, 5855 (2010).
- 7 7 R. Abe, M. Higashi, and K. Domen, *J. Am. Chem. Soc.* 132, 11828 (2010).
- 8 8 M. Higashi, K. Domen, and R. Abe, *Energy Environ. Sci* 4, 4138 (2011).
- 9 9 P. A. Kohl, S. N. Frank, and A. J. Bard, *J. Electrochem. Soc.* 124, 225 (1977).
- 10 10 A. Paracchino, N. Mathews, T. Hisatomi, M. Stefik, S. D. Tilley, and M. Graetzel, *Energy Environ. Sci* 5, 8673 (2012).
- 11 11 W. Siripala, A. Ivanovskaya, T. F. Jaramillo, S. H. Baeck, and E. W. McFarland, *Sol. Energy Mater. Sol. Cells* 77, 229 (2003).
- 12 12 Y. Lin, R. Kapadia, J. Yang, M. Zheng, K. Chen, M. Hettick, X. Yin, C. Battaglia, I. D. Sharp, J. W. Ager, and A. Javey, *J. Phys. Chem. C* 119, 2308 (2015).
- 13 13 D. Yokoyama, T. Minegishi, K. Jimbo, T. Hisatomi, G. Ma, M. Katayama, J. Kubota, H. Katagiri, and K. Domen, *Appl. Phys. Express* 3 (2010).
- 14 14 M. Ichimura, K. Takeuchi, Y. Ono, and E. Arai, *Thin Solid Films* 361, 98 (2000).
- 15 15 K. Omoto, N. Fathy, and M. Ichimura, *Jpn. J. Appl. Phys., Part1* 45, 1500 (2006).
- 16 16 N. Sato, M. Ichimura, E. Arai, and Y. Yamazaki, *Sol. Energy Mater. Sol. Cells* 85, 153 (2005).
- 17 17 J. J. M. Vequizo and M. Ichimura, *Appl. Phys. Express* 6 (2013).
- 18 18 J. J. M. Vequizo and M. Ichimura, *Jpn. J. Appl. Phys.* 52 (2013).
- 19 19 T. Pauporte and D. Lincot, *Appl. Phys. Lett.* 75, 3817 (1999).
- 20 20 T. Pauporte and D. Lincot, *Electrochim. Acta* 45, 3345 (2000).
- 21 21 S. Peulon and D. Lincot, *J. Electrochem. Soc.* 145, 864 (1998).
- 22 22 M. Izaki and T. Omi, *Appl. Phys. Lett.* 68, 2439 (1996).
- 23 23 M. Izaki and T. Omi, *J. Electrochem. Soc.* 144, 1949 (1997).
- 24 24 N. R. Mathews, H. B. M. Anaya, M. A. Cortes-Jacome, C. Angeles-Chavez, and J. A. Toledo-Antonio, *J. Electrochem. Soc.* 157, H337 (2010).
- 25 25 Z. Zainal, M. Z. Hussein, and A. Ghazali, *Sol. Energy Mater. Sol. Cells* 40, 347 (1996).
- 26 26 J. J. M. Vequizo and M. Ichimura, *Jpn. J. Appl. Phys.* 51 (2012).
- 27 27 J. J. M. Vequizo and M. Ichimura, *Appl. Phys. Express* 7 (2014).
- 28 28 W. J. Chun, A. Ishikawa, H. Fujisawa, T. Takata, J. N. Kondo, M. Hara, M. Kawai, Y. Matsumoto, and K. Domen, *J. Phys. Chem. B* 107, 1798 (2003).
- 29 29 I. Goldfarb, D. A. A. Ohlberg, J. P. Strachan, M. D. Pickett, J. J. Yang, G. Medeiros-Ribeiro, and R. S. Williams, *Journal of Physics D-Applied Physics* 46, 6 (2013).
- 30 30 A. Kudo and Y. Miseki, *Chem. Soc. Rev.* 38, 253 (2009).
- 31 31 S. Hu, N. S. Lewis, J. W. Ager, J. Yang, J. R. McKone, and N. C. Strandwitz, *J. Phys. Chem. C* 119, 24201 (2015).
- 32 32 J. Zhao, T. Minegishi, L. Zhang, M. Zhong, Gunawan, M. Nakabayashi, G. Ma, T. Hisatomi, M. Katayama, S. Ikeda, N. Shibata, T. Yamada, and K. Domen, *Angew. Chem. Int. Ed.* 53, 11808 (2014).
- 33 33 S. Hu, M. R. Shaner, J. A. Beardslee, M. Lichterman, B. S. Brunschwig, and N. S. Lewis, *Science* 344, 1005 (2014).

46

47

1



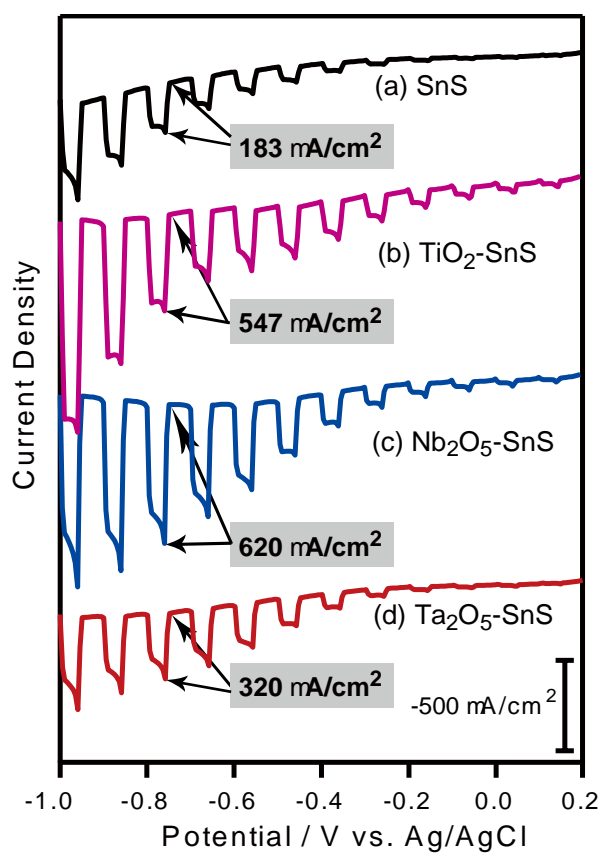
2

3 Figure 1. (a) Photocurrent response of SnS photocathode upon 660 nm intermittent illumination. (b) IPCE curve  
4 of SnS photocathode deposited by 3-step pulsed electrodeposition for 10 min. Electrolyte: 0.1 M  $\text{Na}_2\text{SO}_4$   
5 aqueous solution.

6



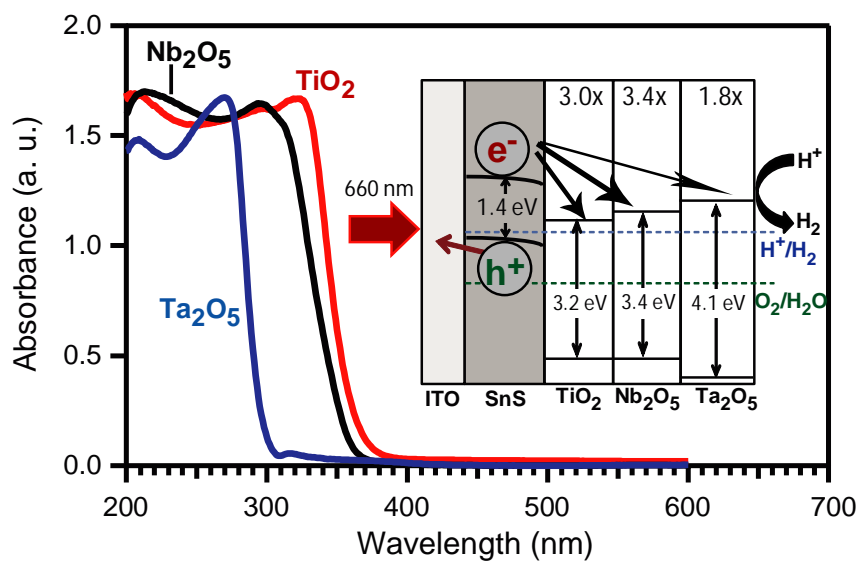
1



2

3 Figure 2. Photoactivity of (a) bare SnS photoelectrode, and SnS coated with different metal oxides: (b) TiO<sub>2</sub>-SnS,  
4 (c) Nb<sub>2</sub>O<sub>5</sub>-SnS, and (d) Ta<sub>2</sub>O<sub>5</sub>-SnS. Electrolyte: 0.1 M Na<sub>2</sub>SO<sub>4</sub> aqueous solution.

5



2

3 Figure 3. UV-Vis diffuse reflectance spectra of  $\text{TiO}_2$ ,  $\text{Nb}_2\text{O}_5$ , and  $\text{Ta}_2\text{O}_5$  films synthesized from the hydrolysis of  
 4 metal chlorides. Inset shows the proposed mechanism of electron migration from SnS to metal oxide coatings  
 5 that results to the enhancement of photocathodic currents.

6